Proceedings of the American Control Conference
San Diego, California • June 1999

INPUT-OUTPUT DATA BASED TRACKING CONTROL*

Alex Babinski
ababinsk@uiuc.edu
Tsu-Chin Tsao
t-tsao@uiuc.edu
Department of Mechanical and Industrial Engineering
University of Illinois at Urbana-Champaign
Urbana, Illinois

Abstract

Traditional methods of tracking controller design involve inverting the system dynamics using the model of the system. Model errors will result in performance degradation and may lead to instability. Since the system parameters vary due to the factors such as age, temperature, etc., there is an interest in tracking control schemes that can efficiently address changes in the system's behavior. This research proposes a tracking control scheme, in which the inverse dynamics of an LTI system are determined using the input-output data. In many practical applications the system is desired to track a set of trajectories that can be characterized by a subspace of L_2. The proposed algorithm utilizes expansion of the output in terms of a signal obtained in an identification experiment by generating a set of vectors spanning the desired subspace. The performance of the scheme is compared with the performance of the conventional model-based feedforward and repetitive controllers.

1 Introduction

The objective of tracking control is to minimize the errors of path following. In a number of applications the desired trajectory is also periodic, like in noncircular turning of engine camshafts that is considered in this paper. In noncircular turning, the radial position of the tool slide is synchronized with the rotation of the spindle, and the cam is produced by following a certain trajectory corresponding to the desired cam shape. The tool trajectories for some of the cams used in the automotive industry are shown in Fig.1. These trajectories share one common feature - they are low frequency signals.

A high performance tracking controller must be used in the tool drive's servocontrol system in order to satisfy stringent profile error requirements for camshafts. The issues involved in tracking controller design are briefly discussed next.

Suppose that a feedback control system that satisfies certain performance requirements with respect to disturbance rejection has already been designed. To minimize tracking errors, the feedback structure is augmented with a feedforward or a repetitive controller (since the desired trajectory is periodic), as shown in Fig.2. The design methods for these schemes are well known. In general, one attempts to find a prefilter that is an approximate inverse of the feedback system, $\Phi = T_{xu}$ (e.g. by pole/zero and phase cancellation, as done in Tomizuka [1987], Tomizuka, *et al.* [1989]). Tracking controllers generate appropriate "modified reference" signal, u, based on the desired trajectory, y^d, or the tracking error, e (in the repetitive control case).

*This work was supported in part by NIST Advanced Technology Program.

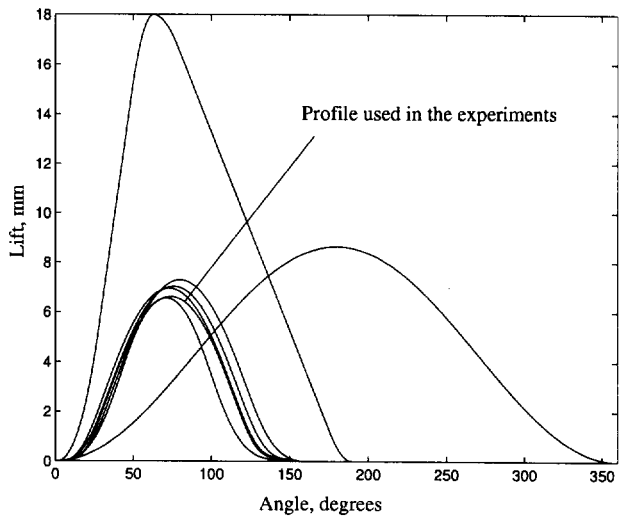

Fig. 1: Cams Used in the Automotive Industry.

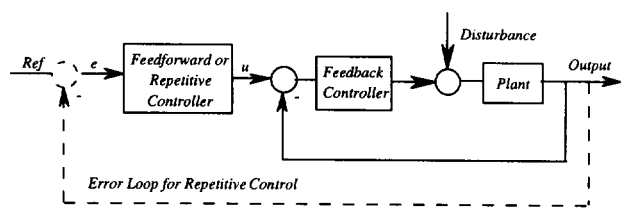

Fig. 2: Control System Configuration.

The necessary control signal, u, can be found by iteration using

$$u_k = u_{k-1} + \gamma \Psi^{-1}(e_{k-1}), \tag{1}$$

where γ is a learning gain, and Ψ^{-1} is an approximate inverse of the inner feedback system mapping, Φ, i.e. $\Phi(\Psi^{-1}(\zeta)) \approx \zeta$. Feedforward control can be viewed as a first iteration in (1). Namely, setting $u_{-1} = 0$, $\gamma = 1$, $e_{-1} = y^d$ leads to

$$u = \Psi^{-1}(y^d), \quad y = \Phi(u) = \Phi(\Psi^{-1}(y^d)) \approx y^d. \tag{2}$$

For the iterative control case, the vector error dynamics are governed by

$$e_k = y^d - \Phi(u_k) = y^d - \Phi(u_{k-1}) - \gamma \Phi(\Psi^{-1}(e_{k-1}))$$

$$\approx \quad e_{k-1} - \gamma e_{k-1} = (1-\gamma)e_{k-1}, \tag{3}$$

and the error converges to zero asymptotically for $0 < \gamma < 2$.

Real systems do not behave exactly like the models that are used for control system design. Unmodeled dynamics and parameter variation due to changes in environment or aging may lead to performance degradation or instability. The model uncertainty is usually larger at higher frequencies, therefore a low-pass filter, Q, is commonly used to improve robustness properties of the repetitive control by suppressing high frequency dynamics in the system (Tsao and Tomizuka [1994]). Adaptive or data based approaches can also be used to reduce or eliminate the need in the exact model of the system. Adaptive feedforward control was considered in Tsao and Tomizuka [1987, 1994]. Design methodology for minimizing feedforward errors using frequency response data was developed in McNab and Tsao [1997]. Messner *et al.* [1991] represented the control signal, necessary to counteract exogenous signals, as an integral of a predefined kernel function multiplied by an unknown influence function. Using time history of the plant, a gradient-like algorithm was used to update the estimate of the influence function. Tao *et al.* [1994] used inverse of a matrix formed from experimental impulse response of the system in conjunction with a scheme similar to (1).

The method proposed in this paper, in effect, eliminates the need in explicit system modeling by determining the inverse system mapping, Ψ^{-1}, using the data from an appropriate system identification experiment. It represents an extension of the ideas contained in previous research on tracking control and is suitable for applications where an LTI system is required to track trajectories from a set characterized by a finite number of frequencies.

Suppose that a signal $h(t)$ is used as an input to the inner feedback system, resulting in an output $g(t)$, as shown in Fig.3. Similar to impulse and impulse response, $h(t)$ and $g(t)$ provide

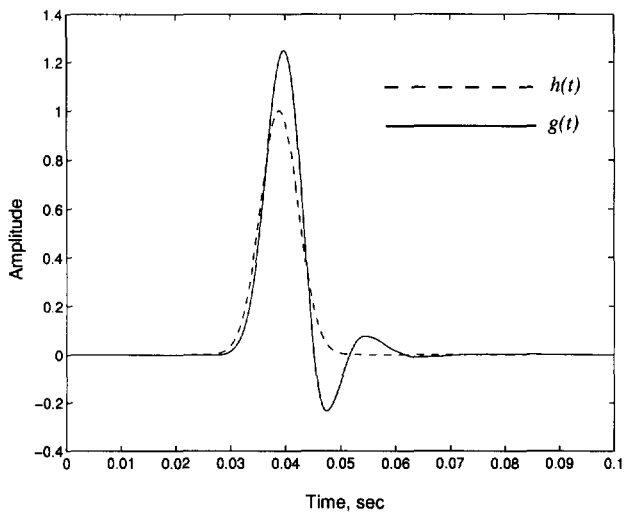

Fig. 3: "System Identification Experiment."

an input-output description of the system dynamics; however, it is limited to the range of frequencies that are contained in $h(t)$. If the desired system output, y^d, can be represented as a linear function of $g(t)$, i.e. $y^d = F[g(t)]$, the input signal to produce this output can be determined as $u = F[h(t)]$. As shown in the following sections, by shifting the experimentally determined signal, $g(t)$, it is possible to generate a nonorthogonal basis set that can be used in conjunction with superposition to represent bandlimited signals, such as the cam profiles shown in Fig.1.

The remainder of the paper is organized as follows. Relevant theoretical results are presented in Section 2. The approach is formalized in Section 3, and experimental results are presented in Section 4. The presentation concludes with discussion in Section 5.

2 System Output Based Function Expansion

Due to the space limitations only sketches of the proofs are provided. It is assumed that all signals are periodic. The notation (f_1, f_2) refers to the inner product in $L_2(0, 2\pi)$:

$$(f_1, f_2) \equiv \frac{1}{2\pi}\int_0^{2\pi} f_1(x)\bar{f}_2(x)\,dx.$$

Suppose $\mathbb{S}$ is a finite dimensional subspace of $L_2(0, 2\pi)$ given by $\mathbb{S} = span\{\phi_n : \phi_n = \frac{1}{\sqrt{2\pi}}e^{inx},\ n = 0, \pm 1, \ldots \pm \frac{N}{2}\}$. Let h be a vector in $\mathbb{S}$, satisfying $(h, \phi_n) \neq 0$ for all n. Assuming that an LTI system Φ does not contain transmission zeros, it follows that

$$g \in \mathbb{S},\ a_n = (g, \phi_n) \neq 0,\ \forall n, \tag{4}$$

where $g = \Phi(h)$. The following theorem provides a function set generated by g that spans $\mathbb{S}$.

Theorem 1

$$span\left\{g_k : g_k = g(x - \frac{2\pi k}{N+1}),\ k = 0, 1, \ldots N\right\} = \mathbb{S}. \tag{5}$$

Proof. $dim\{\mathbb{S}\} = N+1$; therefore, it remains to show that the (N+1) elements of the set $\{g_k\}$ are linearly independent. Functions g_k are LI $\Leftrightarrow \lambda_n(\Gamma) \neq 0,\ \forall n$, where $\lambda_n(\Gamma)$ are eigenvalues of the Grammian

$$\Gamma = \begin{bmatrix} (g_0, g_0) & \cdots & (g_0, g_N) \\ \vdots & \ddots & \\ (g_N, g_0) & \cdots & (g_N, g_N) \end{bmatrix}. \tag{6}$$

Lemma 2

$$\lambda_n(\Gamma) = (N+1)|a_n|^2,\ \ n = 0, \pm 1, \ldots \pm N/2. \tag{7}$$

Proof of Lemma 2. It is straightforward to verify that $(g_i, g_j) = (g_{i+1}, g_{j+1})$ and $(g_N, g_j) = (g_1, g_{j+1})$, i.e. Γ is a circulant matrix. Eigenvalues of circulant matrices are equal to the values of the polynomial, formed from the entries of the first row, evaluated at $N+1$ equally spaced points around a unit circle (Ortega [1987]):

$$\lambda_n(\Gamma) = (g_0, g_0) + (g_0, g_1)\nu_n + (g_0, g_2)\nu_n^2 + \cdots + (g_0, g_N)\nu_n^N \tag{8}$$

where

$$\nu_n = e^{i\frac{2\pi n}{N+1}},\ \ n = 0, \pm 1, \ldots \pm N/2. \tag{9}$$

It follows from (8) that

$$\begin{aligned} \lambda_n(\Gamma) &= (g_0, g_0 + g_1\nu_n + g_2\nu_n^2 + \cdots + g_N\nu_n^N) = \\ &= (g_0, (N+1)a_n e^{inx}) = (N+1)\bar{a}_n(g_0, e^{inx}) = \\ &= (N+1)\bar{a}_n a_n. \quad \square \end{aligned} \tag{10}$$

The second equality in (10) follows from a simple but quite remarkable fact

$$g_0 + g_1\nu_n + g_2\nu_n^2 + \cdots + g_N\nu_n^N = (N+1)a_n e^{inx}, \qquad (11)$$

which can be verified by direct substitution.
Noting (7) and (4), it follows that the grammian, Γ, is nonsingular, which completes the proof of Theorem 1. ■

Theorem 3 *The expansion of a vector $y \in \mathbb{S}$, with respect to the basis set $\{g_k\}$, is given by*

$$y = \sum_{k=0}^{N} \alpha_k g_k = \sum_{k=0}^{N} (y, q_k) g_k, \qquad (12)$$

where $\{q_k\}$ is the dual basis set:

$$q_k = q(x - \frac{2\pi k}{N+1}),\ k = 0, 1, \ldots N \qquad (13)$$

$$q(x) = \frac{1}{N+1} \sum_{n=0}^{\pm N/2} \frac{1}{a_{-n}} e^{nix}, \qquad (14)$$

with the property

$$(g_i, q_j) = \delta_{ij}. \qquad (15)$$

Proof. Given a function $y \in \mathbb{S}$, the vector of expansion coefficients, $\alpha \in \mathbb{R}^{N+1}$ is determined as

$$\begin{bmatrix} \alpha_0 \\ \vdots \\ \alpha_N \end{bmatrix} = \begin{bmatrix} (g_0, g_0) & \cdots & (g_0, g_N) \\ \vdots & \ddots & \\ (g_N, g_0) & \cdots & (g_N, g_N) \end{bmatrix}^{-1} \begin{bmatrix} (g_0, y) \\ \vdots \\ (g_N, y) \end{bmatrix} \qquad (16)$$

The inverse of the Grammian is given by

$$\Gamma^{-1} = UD^{-1}U^*, \qquad (17)$$

where

$$D = (N+1)diag[|a_0|^2, |a_1|^2, |a_2|^2, \ldots, |a_2|^2, |a_1|^2], \qquad (18)$$

and

$$U = \frac{1}{\sqrt{N+1}} \begin{bmatrix} 1 & 1 & 1 & \cdots & 1 \\ 1 & \nu & \nu^2 & \cdots & \nu^N \\ 1 & \nu^2 & \nu^4 & \cdots & \nu^{2N} \\ \vdots & \vdots & \vdots & & \vdots \\ 1 & \nu^N & \nu^{2N} & \cdots & \nu^{N^2} \end{bmatrix} \qquad (19)$$

with $\nu = e^{i\frac{2\pi}{N+1}}$. Substituting these expressions into (16) and collecting terms in conjunction with (11) yields the desired results. ■

In the following, let operator $\Gamma_g^+ : L_2(0, 2\pi) \to \mathbb{R}^{N+1}$ denote the operation in (16), and operator $\Sigma_v : \mathbb{R}^{N+1} \to \mathbb{S}$ denote linear combination of $N+1$ vectors $\{v_k\}$ in $\mathbb{S}$[1].

It can be seen that operator $P_{\mathbb{S}} = \Sigma_g \Gamma_g^+$ is an orthogonal projection of L_2 onto $\mathbb{S}$. Indeed, writing $f \in L_2$ as $f = f_{\mathbb{S}} + f_{\mathbb{S}^\perp}$, it follows that

$$\sum_{k=0}^{N} (f, q_k) g_k = \sum_{k=0}^{N} (f_{\mathbb{S}} + f_{\mathbb{S}^\perp}, q_k) g_k = \sum_{k=0}^{N} (f_{\mathbb{S}}, q_k) g_k$$
$$+ \sum_{k=0}^{N} (f_{\mathbb{S}^\perp}, q_k) g_k = \sum_{k=0}^{N} (f_{\mathbb{S}}, q_k) g_k, \qquad (20)$$

because $q_k \in \mathbb{S}$.

The calculations simplify considerably in discrete domain, where all operations reduce to matrix multiplication. For example, suppose a function $g \in \mathbb{S}$ is given by M discrete points. The operator Σ_g is given by a $M \times N+1$ matrix G, whose columns are copies of g, cyclically shifted by $L = M/(N+1)$:

$$\Sigma_g = G = \begin{bmatrix} g(1) & g(M-L+1) & \cdots & g(M-LN+1) \\ \vdots & \vdots & & \vdots \\ g(M) & g(M-L) & & g(M-LN) \end{bmatrix}. \qquad (21)$$

The operator Γ_g^+ is given by a $N+1 \times M$ matrix

$$\Gamma_g^+ = \left(G^{\mathrm{T}} G\right)^{-1} G^{\mathrm{T}}. \qquad (22)$$

Comment. As can be seen from Theorem 3, the conditioning of the expansion is directly affected by the magnitude of the frequency components in $g(t)$. Since most physical systems exhibit low-pass behavior, in the cases when the frequency content of the desired trajectory is well above the system's bandwidth, special attention must be paid to the design of appropriate excitation function $h(t)$.

3 Input-Output Data Based Tracking Control

The system inverse, necessary for tracking control, can be found by exploiting the fact that $h(t)$ and $g(t) = \Phi h(t)$ contain implicit information about system dynamics in some frequency range.

Theorem 4 *Given a stable LTI system Φ, and two basis sets $\{h_k\}$ and $\{g_k\}$, generated by $h \in \mathbb{S}$ and $g = \Phi h$ respectively, it follows that*

$$\Phi \Sigma_h = \Sigma_g, \qquad (23)$$
$$\Phi \Sigma_h \Gamma_g^+ = P_{\mathbb{S}}, \qquad (24)$$
$$\Gamma_g^+ \Phi \Sigma_h = I. \qquad (25)$$

An easy proof utilizes LTI properties of Φ.

It follows from (24) that the system inverse over $\mathbb{S}$ is given by

$$\Psi^{-1} = \Sigma_h \Gamma_g^+. \qquad (26)$$

Thus, for the desired trajectory, y^d, the required feedforward input is calculated (in discrete time) as

$$u = H \left(G^{\mathrm{T}} G\right)^{-1} G^{\mathrm{T}} y^d, \qquad (27)$$

where H and G are matrices, whose columns are cyclically shifted copies of h and g respectively, as given in (21).

In the iterative scheme, let the control signal $u(t)$ be constrained to $\mathbb{S}$. Noting (26), the control law (1) is given by

$$u(k) \equiv \Sigma_h w(k) = \Sigma_h w(k-1) + \gamma \Sigma_h \Gamma_g^+ e(k-1). \qquad (28)$$

Using linearity of Γ_g^+, the control system, shown in Fig.4a[2], can be redrawn as shown in Fig.4b. From property (25), it follows that the plant becomes an identity, as indicated in the picture. It can be seen that the control law

[1] With this notation, the basis expansion (12) can be compactly written as $y = \Sigma_g \Gamma_g^+(y)$.

[2] For simplicity, the disturbance signal enters the system at the plant output.

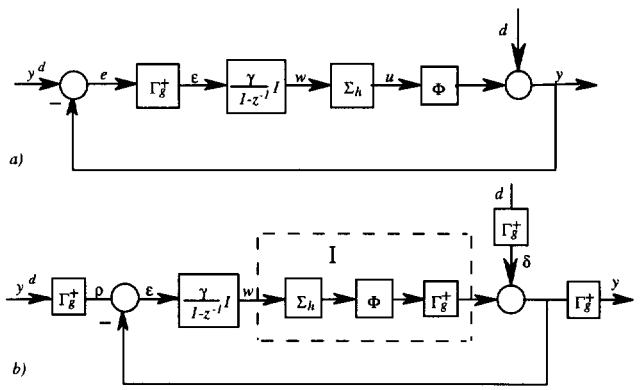

Fig. 4: a) Iterative Control System. b) Equivalent Structure.

$$w(k) = w(k-1) + \gamma\varepsilon(k-1), \quad \varepsilon(k-1) = \Gamma_g^+ e(k-1), \quad (29)$$

guarantees asymptotic converges of the error to zero in $\mathbb{S}$:

$$\begin{aligned} \varepsilon(k) &= \rho - w(k) - \delta = \rho - w(k-1) - \gamma\varepsilon(k-1) - \delta = \\ &= \varepsilon(k-1) - \gamma\varepsilon(k-1) = (1-\gamma)\varepsilon(k-1), \end{aligned} \quad (30)$$

where $\rho, \delta, \varepsilon, w \in \mathbb{R}^{N+1}$ are as shown in Fig.4b. It follows that the steady state error is given by

$$e_{ss} = y^d_{\mathbb{S}^\perp} - d_{\mathbb{S}^\perp}. \quad (31)$$

4 Experimental Results

The experimental system consisted of a linear tool slide driven by a voice coil actuator. A laser sensor with 0.628 μm resolution was used for measuring the position of the tool. The control algorithm was implemented on a 133 MHz Pentium computer and a DSP board with Texas Instruments TMS320C32 floating point digital signal processor. The host program was used for communication with the the DSP, and to conduct necessary on-line calculation for tracking control. The feedback control algorithm and data collection were done by the DSP at a sampling frequency of $5kHz$. Spindle speed of $600rpm$ and the cam profile indicated in Fig.1 was used as a desired trajectory (corresponding to the base period $T = 0.1sec$, and the maximum tool travel, velocity, and acceleration of $6.5mm$, $0.6m/sec$, and $98.2m/sec^2$ respectively). An aggressive $\mathcal{H}_\infty$ feedback controller was designed to provide adequate disturbance rejection characteristics for the drive. A noncausal feedforward and repetitive controllers were also designed (Tsao [1994], Tomizuka *et al.* [1989]) to be compared with the proposed data based scheme. Signal vectors contained 500 data point ($M = 500$); in order to reduce the computation time for control update in the iterative scheme, every 10^{th} data point of the $g(t)$ and $e(t)$ was used ($M_g = M_e = 50$, which corresponds to the Nyquist frequency of $250Hz$).

The frequency spectrum of the desired trajectory for the given base period, $T = 0.1sec$, is shown in Fig.5. Since the signal strength is very small above $120Hz$ (i.e. 12 harmonics), the expansion set with $N + 1 = 2 \times 12 + 1 = 25$ should be sufficient to achieve low tracking errors. The following ad hoc procedure was used for the design of the signal $h(t)$ used in the system identification. A Gaussian distribution,

$$h(t) = e^{-\frac{t^2}{\sigma^2}}, \quad (32)$$

is a convenient form for the "impulse-like" function, whose frequency content is easily controlled by varying σ. The parameter was reduced until the 25×25 matrix $\Gamma_g = G^T G$, formed using the $g(t)$ data obtained in the experiment, became well conditioned. Time and frequency domain plots of signals $h(t)$ and $g(t)$ are shown in Fig.3 and Fig.5 respectively. It should be noted that these signals are not bandlimited, although the high frequency components are small. Results of extensive simulation and experimental tests show that the performance of the scheme is not affected by these components. The work on theoretical characterization of the introduced error is in progress.

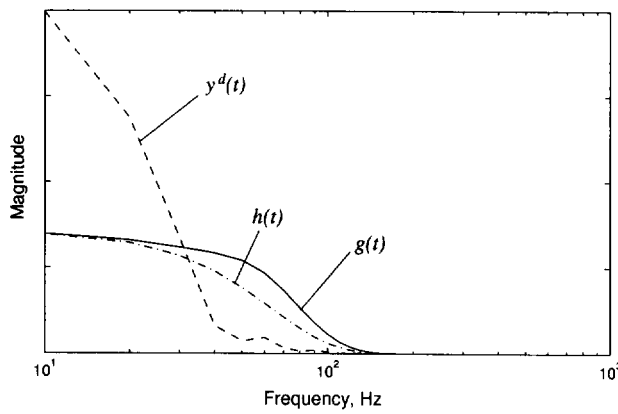

Fig. 5: Power Spectrums of the Desired Trajectory and the Basis Functions (DFT).

The feedforward control signal was calculated as $u_{ff} = \Sigma_h \Gamma_g^+ y^d = H(G^T G)^{-1} G^T y^d$. The tracking errors observed in the experiments are compared with the errors of model-based feedforward controller in Fig.6 for two amplitudes of the desired trajectory. The degradation of performance with increasing amplitude can be attributed to the inability of the system description to cover a wider operating range. Error feedback used in the iterative control significantly improves tracking performance, as can be seen in Fig.7 and Fig.8.

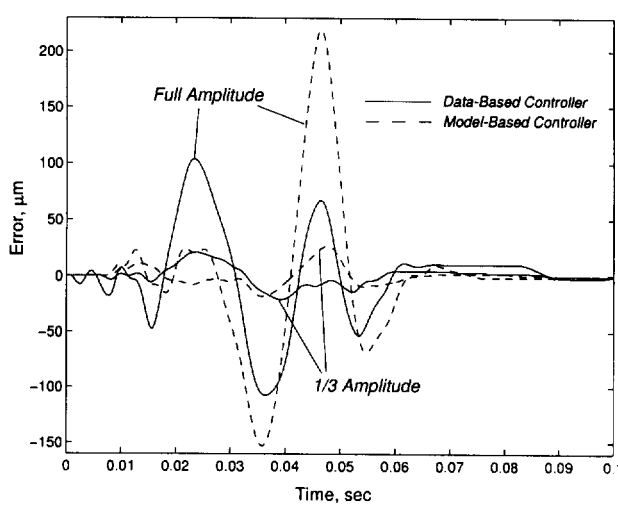

Fig. 6: Tracking Error with Feedforward Control.

The control signal in the iterative control scheme was calculated on the host computer as $u_{il} = \Sigma_h(w(k-1) + \gamma\Gamma_g^+ e(k-$

1)) = $H(w(k-1) + \gamma(G^TG)^{-1}G^Te(k-1))$. The calculation of the control signal (written in C) and data transfers between the host and the DSP board took approximately $5msec$ (25 sampling intervals), which was slightly longer than the time available for update at the end of the cycle (equal to M/M_g, or 10 sampling intervals). Therefore, a "delayed" scheme was used, where the update of u_{il} was performed every two cycles.

Figure 7 shows the convergence of the tracking error with $\gamma = 0.9$ for full amplitude cam profile. As expected, the frequency of the steady state error is outside the $120Hz$ range, as can be seen in Fig.8. The figure also shows the steady state error achieved with the model-based repetitive control.

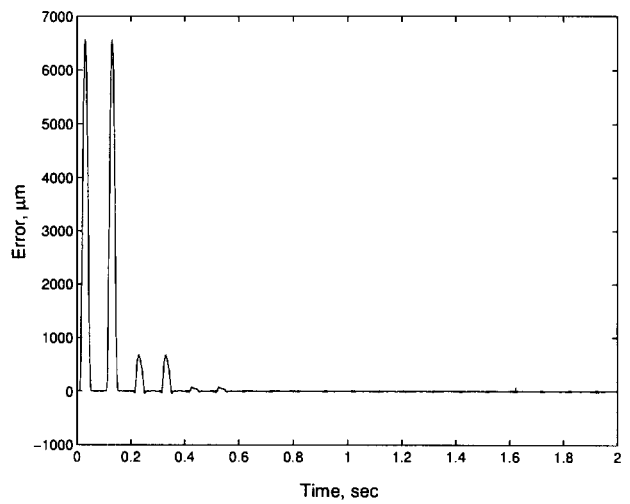

Fig. 7: Convergence of the Tracking Error. $\gamma = 0.9$.

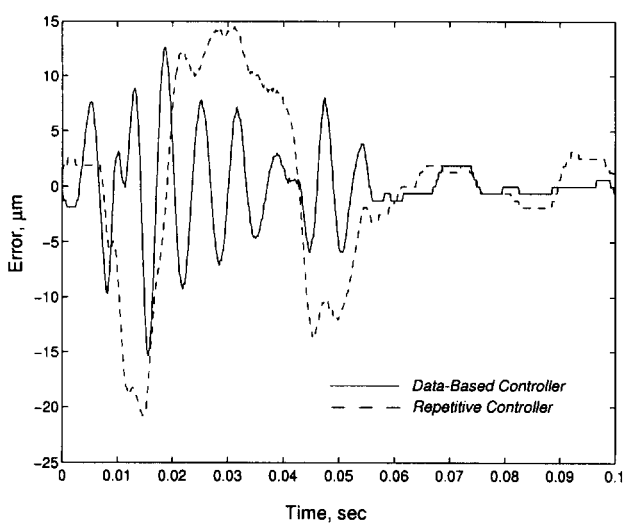

Fig. 8: Steady State Tracking Error.

5 Conclusion

An approach to tracking control based on the implicit system inversion over a finite dimensional subspace of $L_2(0, 2\pi)$ was presented. Experimental results show that the performance of the proposed scheme is comparable with the conventional model-based methods. The method utilizes the data from a single identification experiment, and therefore is of value for applications, where the system parameters may vary during operation, but extensive modeling is not practical or feasible. In certain sense the scheme is similar to an impact hammer test, and by controlling the frequency content of the input function it is possible to focus only on the dynamics that are essential for tracking a given set of trajectories. Expansion of the error and control signals in terms of the low frequency basis functions has an affect of suppressing high frequency dynamics, which improves the robustness of the iterative PI scheme.

References

[1] McNab, R.J., and Tsao, T.-C., 1997, "Frequency Response Based Feedforward Control Design with Uncertainty Considerations," *Proceedings of the American Control Conference,* Vol. 5, pp. 2726-2730.

[2] Ortega, S., 1987, *Matrix Theory.* Plenum Press, New York, NY.

[3] Tao, K.M., Kosut, R.L., Aral, G., 1994, "Learning Feedforward Control," *Proceedings of the American Control Conference,* Vol. 3, pp. 2575-2579.

[4] Tomizuka, M., 1987, "Zero Phase Error Tracking Algorithm for Digital Control," *ASME Journal of Dynamic Systems, Measurement, and Control,* Vol. 109, pp. 65-68.

[5] Tomizuka, M., Tsao, T.-C., Chew, K.-K., 1989, "Analysis and Synthesis of Discrete-Time Repetitive Controllers," *ASME Journal of Dynamic Systems, Measurement, and Control,* Vol. 111, pp. 353-358.

[6] Tsao, T.C., and Tomizuka, M., 1987, "Adaptive Zero Phase Error Tracking Algorithm for Digital Control," *ASME Journal of Dynamic Systems, Measurement, and Control,* Vol. 109, pp. 349-354.

[7] Tsao, T.-C., 1994, "Optimal Feed-Forward Digital Tracking Controller Design," *ASME Journal of Dynamic Systems, Measurement, and Control,* Vol. 116, pp. 583-592.

[8] Tsao, T.-C., and Tomizuka, M., 1994, "Robust Adaptive and Repetitive Digital Tracking Control and Application to a Hydraulic Servo for Noncircular Machining," *ASME Journal of Dynamic Systems, Measurement, and Control,* Vol. 116, pp. 24-32.